Demixing, surface nematization, and competing adsorption in binary mixtures of hard rods and hard spheres under confinement

Liang Wu, Alexandr Malijevský, Carlos Avendaño, Erich A. Müller, and George Jackson

Citation: J. Chem. Phys. **148**, 164701 (2018); doi: 10.1063/1.5020002
View online: https://doi.org/10.1063/1.5020002
View Table of Contents: http://aip.scitation.org/toc/jcp/148/16
Published by the American Institute of Physics

Demixing, surface nematization, and competing adsorption in binary mixtures of hard rods and hard spheres under confinement

Liang Wu,[1,2] Alexandr Malijevský,[3,4] Carlos Avendaño,[5] Erich A. Müller,[1] and George Jackson[1]

[1]*Department of Chemical Engineering, Imperial College London, South Kensington Campus, London SW7 2AZ, United Kingdom*
[2]*School of Chemistry and Chemical Engineering, Shanghai Jiao Tong University, Shanghai 200240, China*
[3]*Department of Physical Chemistry, University of Chemical Technology Prague, 166 28 Praha 6, Czech Republic*
[4]*Department of Microscopic and Mesoscopic Modelling, ICPF of the Czech Academy of Sciences, 165 02 Prague 6, Czech Republic*
[5]*School of Chemical Engineering and Analytical Science, The University of Manchester, Sackville Street, Manchester M13 9PL, United Kingdom*

(Received 19 December 2017; accepted 23 March 2018; published online 23 April 2018)

A molecular simulation study of binary mixtures of hard spherocylinders (HSCs) and hard spheres (HSs) confined between two structureless hard walls is presented. The principal aim of the work is to understand the effect of the presence of hard spheres on the entropically driven surface nematization of hard rod-like particles at surfaces. The mixtures are studied using a constant normal-pressure Monte Carlo algorithm. The surface adsorption at different compositions is examined in detail. At moderate hard-sphere concentrations, preferential adsorption of the spheres at the wall is found. However, at moderate to high pressure (density), we observe a crossover in the adsorption behavior with nematic layers of the rods forming at the walls leading to local demixing of the system. The presence of the spherical particles is seen to destabilize the surface nematization of the rods, and the degree of demixing increases on increasing the hard-sphere concentration. https://doi.org/10.1063/1.5020002

I. INTRODUCTION

Particle shape is one of the most important features governing the collective behavior of colloidal suspensions.[1,2] As the shape of particles deviates from spherical geometry, a rich phase behavior emerges due to the additional orientational degrees of freedom giving rise to a variety of complex crystal, plastic crystal, and liquid crystal (LC) structures.[3–7] Colloidal particles are also appealing as model systems to study various physical phenomena due to the possibility of controlling the range, strength, and form of the interparticle interactions, allowing for the design of interactions that are purely repulsive at short range, i.e., approaching the hard-core interaction limit.[8] In his pioneering work of 1949, Onsager[9] offered a successful explanation for the isotropic-nematic phase transition observed in uniaxial anisotropic particles such as thin rods modeled as hard spherocylinders: cylinders of diameter D and length L capped at each end by hemispheres of diameter D. Onsager described the isotropic-nematic phase transition as a competition between the orientational entropy, which favours the stabilization of isotropic phases, and the packing (free-volume) entropy which induces the alignment of the particles thus promoting the formation of nematic phases. Onsager's second-virial theory provides a good description of rod-like particles in the limit of extreme shape anisotropies corresponding to $L/D \to \infty$ in the case of HSCs.[10] As the aspect ratio L/D of the particles is decreased, the theory becomes less reliable, and more accurate methods such as higher-order density functional theories (DFTs)[11,12] and computer simulations[10,13] are required to accurately describe the ordering transitions.

The phase behavior of non-spherical particles becomes even more complex in the presence of external potentials such as electromagnetic fields, gravity, and geometric confinement.[14] The behavior of rod-like particles in contact with solid substrates modeled as hard structureless walls has been studied extensively.[15–17] The broken spatial symmetry along the normal direction to the wall induces additional phenomena such as anchoring (see Ref. 16 for a review), in which the orientation of the particles at the wall is different to that in the bulk system; in some cases, the extent of surface orientation may be of a macroscopic dimension. The influence of the alignment of the particles at the wall on the isotropic-nematic transition has been studied theoretically using a variety of approaches including phenomenological Landau-de Gennes theory,[18] mean-field DFT,[19–21] and generalized Onsager theory.[22–25] A second-virial Onsager theory has been employed by van Roij *et al.*[26] to study confined rectangular rods in which the orientations of the particles are restricted to three possible directions (the Zwanzig model): a continuous uniaxial-biaxial nematic surface phase transition was found for the isotropic fluid in contact with a single planar hard wall, followed by wetting of the wall by a nematic film comprising particles oriented parallel to the wall corresponding to homogeneous

(planar) alignment. The appearance of the nematic film was found to occur before the phase transition to a bulk nematic phase away from the wall. A first-order capillary nematization transition was observed when the fluid was confined between two parallel hard walls, with a capillary critical point for wall interseparations of about twice the length of the rods. Using a similar model, Aliabadi *et al.*[27] showed that the width of the nematic film diverges logarithmically as the density of the systems approaches the isotropic-nematic transition. The effect of confinement on the positional order and smectic layering of aligned hard cylinders has also been studied using the Onsager free-energy functional.[28] More recently, surface induced phase transitions exhibited by semi-flexible polymer chains confined between two parallel walls have been studied using a self-consistent field theory.[29] Despite these efforts, an accurate theoretical description of liquid crystalline ordering near solid surfaces remains very challenging (see Ref. 30 for a recent review).

Computer simulation studies of various types of non-spherical particles either under confinement or in the presence of a solid substrate have been reported for a wide variety of model systems including: hard spherocylinders,[31–36] hard needles,[25] hard ellipsoids,[37,38] hard cut spheres,[35,39] spherical caps,[40] hard dimers,[41] hard Gaussian overlap particles,[42] Gay-Berne particles,[43–46] and board-like Zwanzig models,[26] as well as systems of spherical particles with an anisotropic Lennard-Jones potential,[47] semiflexible polymer chains,[48–51] and rod-like particles with chiral interactions.[52,53] Several types of surface-particle potentials and heterogeneities including surface roughness,[54] softness,[39] surface anchoring,[17] competing walls,[55] and spherical confinement[56] have also been examined in simulations of confined liquid crystals. In particular, the studies of Mao *et al.*[32] and Dijkstra *et al.*[33] provide an excellent analysis of the adsorption, structure, and orientation of hard spherocylinders at hard surfaces. Mao *et al.*[32] reported Monte Carlo (MC) simulations of hard spherocylinders (with aspect ratios of L/D = 10 and 20) confined between two parallel hard structureless walls for states of relatively low density; the emphasis of their work was understanding the depletion forces induced by the walls, the surface adsorption, and a quantification of the surface tension for the isotropic fluid in contact with the wall. In their thorough simulation study, Dijkstra *et al.*[33] examined the behavior of hard spherocylinders in contact with a single wall (allowing the thickness of the nematic film to diverge) investigating the surface adsorption and nematization of particles with an aspect ratio of L/D = 15. Simulation studies of the hard spherocylinders with L/D = 10 confined between two impenetrable parallel hard walls have been carried out to determine the profiles of the number density, nematic order parameter, degree of biaxiality, and normal and tangential components of the pressure tensor which allow one to obtain the fluid-wall interfacial tension of the system deep into the liquid-crystalline region.[57,58] Savenko and Dijkstra[59] also analyzed the sedimentation and phase equilibria of hard spherocylinders on a planar hard wall observing the formation of nematic, smectic, and even crystal phases.

From the experimental perspective, liquid-crystalline phases observed in suspensions of colloidal particles such as vanadium pentoxide (V_2O_5),[60] gibbsite [$Al(OH)_3$] platelets,[61,62] carbon nanotubes,[63] and some biological systems such as protein fibers,[64] tobacco mosaic virus,[65] *fd*-virus,[66,67] polypeptide solutions,[68,69] and DNA chains[70] offer convenient test beds for an assessment of the simple hard-core models of mesogenic systems. The work by Galanis *et al.*[71] provides a very useful insight into the surface behavior of granular rod-like particles (with an aspect ratio of $L/D \sim 20$) for very thin layers of rods in a quasi-2D circular container. The measured number density profiles are in excellent agreement with previous findings from computer simulation. The influence of a flat wall on the surface anchoring of colloidal rods has been examined for aqueous suspensions of silica particles.[72] As with other colloidal systems of this type, the silica rods exhibit a similar behavior to the athermal (purely repulsive) system and are of sufficiently low polydispersity to allow for the formation of nematic and smectic phases with increasing particle concentration. Good agreement is found with corresponding results obtained from computer simulations of hard spherocylinders.[10,11,13,73–76] This interesting work provides experimental confirmation that rod-like particles adopt a planar anchoring configuration in the vicinity of the surface. In these experimental analogues of the hard-core system, the effect of the surface spans over tens of microns.

Besides the aforementioned studies dealing with one-component liquid-crystalline systems, there is a large body of work devoted to modeling and understanding the phase behavior of athermal mixtures of mesogenic components including rod-rod,[67,77–80] rod-sphere,[81–91] rod-disc,[92–99] disc-disc,[100,101] and disc-sphere[102] hard-core systems. The reader is directed to Ref. 103 for a more detailed discussion. Although theoretical studies of binary mixtures of rod-like and spherical particles in the presence of structureless solid substrates have been reported,[85,104] computer simulation studies of rod-sphere mixtures under confinement in the form of a slit pore are scarce.[91]

It is the purpose of our current paper to fill this gap. Here, we study the adsorption behavior of binary mixtures of hard spheres and hard spherocylinders confined by a parallel hard wall using Monte Carlo simulation. This model system is entirely athermal so that its properties are governed by purely entropic effects. In our previous work,[91] we described the isotropic-nematic phase behavior of the mixture in bulk. We now assess the effect of hard walls on formation of nematic films at conditions where only an isotropic phase is stable in the bulk. In particular, we examine the trade-off between the stabilization of the nematic phase by the presence of the wall and the destabilizing effect of the hard spheres on the orientational order of the system.

II. SIMULATION DETAILS

The methodology employed in our current work is similar to that described in a previous paper.[91] Binary mixtures of hard spherocylinders (HSC) and hard spheres (HS) confined between two hard walls are studied using constant normal-pressure Monte Carlo (NP_NT-MC) simulations, where N is the total number of particles, P_N is the normal pressure (directed

perpendicular to the wall), and T is the absolute temperature. Strictly speaking, the surface area A and the global composition of the mixture should be included in the designation of the ensemble but we choose to retain the NP_NT abbreviation for conciseness, bearing in mind that the area and composition are also kept constant. Throughout our simulations, the number of hard spherocylinders with an aspect ratio of $L/D = 5$ is fixed at $N_{HSC} = 1482$, while the number of hard spheres N_{HS}, of diameter D, is varied to specify the hard-sphere mole fraction (composition) given by $x_{HS} = N_{HS}/N$ where $N = N_{HS} + N_{HSC}$.

The geometry of the simulation setup is shown in Fig. 1. We consider a rectangular simulation box with standard Cartesian coordinates oriented along the box edges. Two parallel hard structureless walls are positioned at $z = 0$ and $z = L_z$ along the z axis and standard periodic boundary conditions are applied along the x and y directions. The volume of the system is allowed to fluctuate during the NP_NT-MC simulations by varying the dimension of the z axis (L_z), while the dimensions of the system along the x and y axes ($L_x = L_y = 25D$) are kept fixed. For systems with this planar symmetry, the condition of mechanical equilibrium ($\nabla\cdot\mathbf{P} = 0$) requires that the normal component of the pressure tensor is constant throughout the sample, and as a consequence the normal component is also equivalent to the equilibrium pressure of the system. With N_{HSC} fixed, we choose the following thermodynamic parameters to define a given system: the composition x_{HS}, the normal pressure P_N, and the surface area of the x–y plane ($A = L_xL_y = 625D^2$).

The NP_NT-MC simulations are performed for 5×10^6 cycles to equilibrate the system and $5–8 \times 10^6$ cycles to accumulate the ensemble averages. Each MC cycle consists of N attempts to displace (and rotate in the case of the hard spherocylinders) a randomly chosen molecule and one trial volume change in which the z dimension is scaled. The breaking of symmetry caused by the hard walls leads to inhomogeneous positional and orientational distributions of the particles along the z axis. In order to evaluate the one-body number density profile $\rho_i(z)$, for $i = \{\text{HS, HSC}\}$, the composition profile $x_i(z)$, and the nematic order parameter profile $S_2(z)$, the simulation box is divided into $j = 1$ to n_{bin} bins of equal width δz along the z direction. The (dimensionless) density profile $\rho_i(z)$ is calculated as

$$\rho_i(z) = \frac{\langle N_i(z)\rangle D^3}{L_xL_y\delta z} \quad \text{for} \quad i = \{\text{HS, HSC}\}, \tag{1}$$

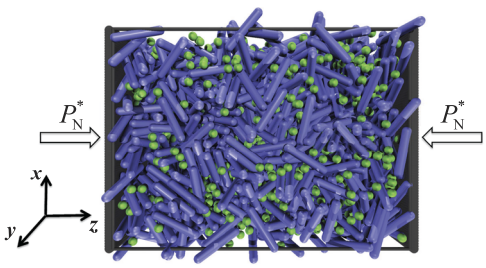

FIG. 1. Geometry and simulation setup used in our NP_NT Monte Carlo simulations to study binary mixtures of hard spherocylinders (blue) and hard spheres (green) confined between two hard walls. The parallel hard walls are placed along the z axis and the equilibrium (normal) pressure P_N is applied perpendicularly to the walls.

where $\langle N_i(z)\rangle$ represents the ensemble average of the local number of particles of component i at position z. Typically $n_{bin} = 200$ bins are used for the calculations. The local composition profile $x_i(z)$ of the mixture is determined as

$$x_i(z) = \frac{\rho_i(z)}{\rho_{HS}(z) + \rho_{HSC}(z)} \quad \text{for} \quad i = \{\text{HS,HSC}\}. \tag{2}$$

Provided the system is sufficiently large, one expects that the structural and thermodynamic properties determined from the central part of the box are consistent with the corresponding bulk limits. In particular, the density profiles $\rho_{HSC}(z)$ and $\rho_{HS}(z)$ are expected to reach the values of the corresponding bulk densities of $\rho_{HSC,b}$ and $\rho_{HS,b}$ far away from the wall. Having determined the bulk densities, the (dimensionless) adsorption Γ_i for each component can be quantified from the following integral:

$$\Gamma_i = \frac{1}{D}\int_0^{L_z} [\rho_i(z) - \rho_{i,b}]\mathrm{d}z \quad \text{for} \quad i = \{\text{HS, HSC}\}. \tag{3}$$

It is important to note that in the case of our confined system, the overall volume of the system is defined to include the two regions inaccessible to the hard particles in layers of thickness $D/2$ close to the two walls.

The orientational order of the hard-spherocylindrical rods is quantified using the average of the second Legendre polynomial S_2[105] of the relative orientation of the principle axis of the particles with respect to the nematic director. The nematic order parameter profile $S_2(z)$ is obtained by determining the Saupe ordering tensor $\mathbf{Q}(j)$ in each bin j,

$$\mathbf{Q}(j) = \left\langle \frac{1}{2N_{HSC,j}} \sum_{i=1}^{N_{HSC,j}} (3\hat{\omega}_i \otimes \hat{\omega}_i - \mathbf{I}) \right\rangle, \tag{4}$$

where $\hat{\omega}_i$ is the orientation of rod i, $N_{HSC,j}$ is the number of hard spherocylinders in bin j, and $\mathbf{I}$ is the unit tensor. On diagonalization of the $\mathbf{Q}(j)$ tensor,[106] three eigenvalues are obtained and the largest value is defined as the local nematic order parameter $S_2(z)$ associated with bin j. Some care should be taken with the calculation of the order-parameter profile due to finite-size effects. Eppenga and Frenkel[107] have shown that the value of the order parameter depends on the number of mesogenic particles, such that the system-size effect in the local order parameter is proportional to $1/(\sqrt{N_{HSC}/n_{bin}})$. If we consider $n_{bin} = 200$ histogram bins, equivalent to the number of bins used in our calculations of the density profiles, the average number of hard spherocylinders present in each bin is $(1482/200) \sim 7$ leading to a large system-size error of ~0.37 in the local order parameter. One can address this problem using a rescaling procedure for $S_2(z)$ in terms of $S_{2,\infty}(z)$ for the infinite system,[108] or simply by enlarging the simulation box at the cost of increasing the computational time. We opt instead to reduce the number of bins to $n_{bins} = 20$, corresponding to a lower finite-size error in the calculated local order parameter of ~ 0.11.

Throughout our work, the thermodynamic variables are expressed in dimensionless units: pressure $P_N^* = P_ND^3/(k_BT)$, and number density $\rho = ND^3/V$.

III. RESULTS AND DISCUSSION

A. Pure hard spherocylinders in planar confinement between hard walls

We first discuss our findings for the phase behavior of pure hard spherocylinders with an aspect ration of $L/D = 5$ in planar confinement between parallel structureless hard walls over a wide range of equilibrium pressures (normal component of the pressure tensor) up to conditions where the bulk isotropic-nematic phase transition is found. The local density near the hard wall in the low-pressure range of $P^*_N = [0.001 - 0.1]$ is shown in Fig. 2(a). At a pressure of $P^*_N \sim 0.02$, a peak in the density profile emerges at $z \sim 3D$, with the maximum of the peak becoming progressively more pronounced as the pressure is increased. The appearance of this peak is explained by the fact that for these low-density states, hard spherocylinders with an aspect ratio of $L/D = 5$ maintain their orientational freedom at $z \sim 3D$, which corresponds to half of the total length $L + D$ of the particles.[31,32] In this low-pressure regime, the wall is depleted (dewetted) of the rod particles. The evolution of the density profiles at higher pressures, corresponding to the range $P^*_N = [0.2 - 1.2]$, is shown in Fig. 2(b). The amplitude of the first peak at $z \sim 3D$ decreases while a new peak near $z \sim D/2$ emerges and quickly becomes the dominant feature of the density profile as P^*_N is increased. The peak near $z \sim D/2$ indicates an increasing adsorption of the rods at the wall corresponding to planar anchoring in the first wetting layer. For this pressure interval, a second wetting layer is also observed between $z \sim 3D/2$ and $\sim 5D/2$, and the maximum of this peak moves closer to the wall as the pressure is increased indicating that the adsorbed rods are parallel to the wall. The formation of the wetting layer appears to be continuous in this case. For strongly attractive walls, one would expect the layering transition near the wall to be first-order, followed by the bulk isotropic-nematic transition.

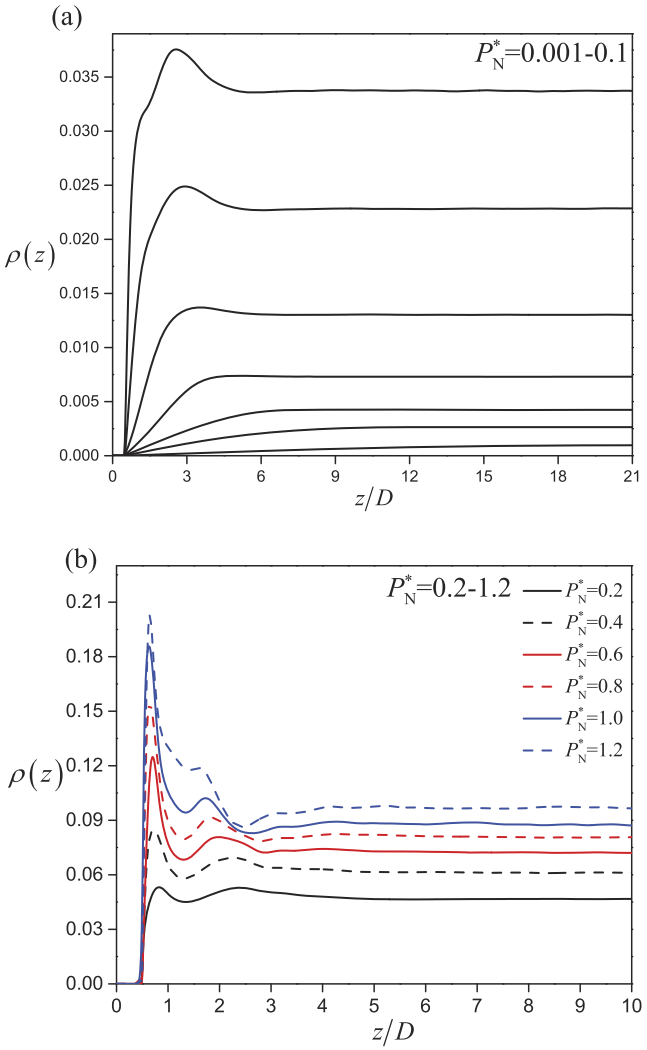

FIG. 2. Density profiles $\rho(z)$ for a system of pure $L/D = 5$ hard spherocylinders confined between parallel hard walls obtained from NP_NT-MC simulations along the normal direction to the wall. The curves correspond to equilibrium (normal) pressures of (from bottom to top): (a) $P^*_N = [0.001, 0.003, 0.005, 0.01, 0.02, 0.05, 0.1]$, and (b) $P^*_N = [0.2 - 1.2]$ in increments of $\Delta P^*_N = 0.2$.

In order to get deeper insight into the structure of the hard spherocylinders near the wall, the local order parameter $S_2(z)$ is calculated as a function of the normal distance z (see Fig. 3). We choose $S_2(z) < 0.4$ to represent a disordered state and $S_2(z) > 0.4$ to represent a local nematic-like state in similar manner as for bulk phases;[11] though one would expect non-zero values of the nematic order parameter even for isotropic states due to finite-size effects, this precise choice is somewhat arbitrary. For a pressure of $P^*_N > 0.8$, the peak in $S_2(z)$ close to the wall in Fig. 3 is associated with a local surface-induced nematization. As the pressure is further increased, the amplitude of the peak also increases indicating the expected enhancement of the orientational ordering of the rods at the wall.

We can distinguish three density (pressure) regimes for the pure component hard spherocylinders near the hard wall. In the low-density regime, corresponding to the pressure range of $P^*_N \sim [0.001 - 0.01]$, the density profiles increase monotonically before reaching the bulk density plateau. This behavior is expected since at low densities, the hard rods maximize their orientational entropy when they are away

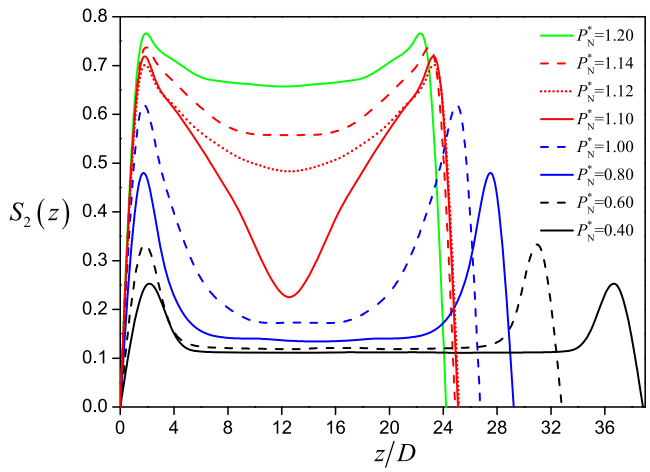

FIG. 3. Nematic order parameter profiles for a system of pure $L/D = 5$ hard spherocylinders confined between parallel hard walls obtained from NP_NT-MC simulations. The curves correspond to equilibrium (normal) pressures in the range $P^*_N = [0.4 - 1.2]$ (from bottom to top).

from the repulsive wall. For moderate densities, corresponding to the pressure range of $P_N^* \sim [0.02 - 0.4]$, the interplay between the orientational entropy and packing effects gives rise to a non-monotonic behavior of the density profile with a pronounced maximum at $\sim(L + D)/2 = 3D$ beyond which the rods are free to rotate. The third regime seen at higher bulk densities, corresponding to the pressure range of $P_N^* \sim [0.6 - 1.2]$, is characterized by surface nematization with the nematic director parallel to the wall. This surface wetting is indicated by the shift of the first maximum in the density profile to $z \sim D/2$. The second maximum located at $z \sim 2D$ is associated with the enhanced orientation of the rods (S_2 is large in this region), in contrast with what is found for the hard-sphere fluid in which case the second maximum lies at $z \sim 3D/2$.[109–111]

From Fig. 3 we can also observe a marked growth in the nematic order parameter in the central part of the system which occurs between $P_N^* = 1.10$ and $P_N^* = 1.14$. Although we cannot rule out that the nematization of the central region is (to a minor degree) affected by capillary effects, we associate this orientational ordering with the bulk isotropic-nematic transition of the system; the corresponding values of the bulk densities for the coexisting isotropic and nematic states are $\rho_{iso} = 0.0867$ and $\rho_{nem} = 0.0941$, respectively. This result is consistent with our previously reported data[91] and also with the values from an earlier study[11] ($P^* = 1.19$, $\rho_{iso} = 0.0914$, and $\rho_{nem} = 0.0932$) obtained with isobaric-isothermal *NPT*-MC simulations for systems of pure hard spherocylinders with an aspect ratio of $L/D = 5$. The isotropic-nematic transition in the confined system is seen to occur at a slightly lower pressure (density) compared to the bulk unconfined system, indicating a small degree of capillary stabilization.

The dependence of the adsorption of hard spherocylinders on the equilibrium (normal) pressure is shown in Fig. 4. In the low-pressure regime ($P_N^* = 0.001 - 0.08$), the system is seen to primarily maximize its orientational entropy which results in the depletion of rod particles from the vicinity of the wall. It is apparent from Fig. 2(a) that for this low-pressure regime, the density profiles significantly differ from the corresponding bulk density limit only in the close vicinity of the wall where the local density is almost zero; a randomly oriented particle is unlikely to be accommodated in this region. The only significant contribution to the adsorption in this region is proportional to $-\rho_b L_w$ where $L_w \sim (L + D)/2$ is the approximate dimension of the depleted region near the wall. The adsorption exhibits a minimum at $P_N^* \sim 0.08$ beyond which we observe a near linear grow up to the isotropic-nematic transition. This can again be understood on the basis of our previous results. In this regime, local surface nematization occurs corresponding to an enhancement in the surface adsorption at the contact density $\rho(D/2)$ which is proportional to P_N according to the contact theorem. Finally, the formation of the bulk nematic phase leads to an abrupt reduction in adsorption as a result of the increase in the bulk density.

We conclude the analysis of pure hard spherocylinders by discussing some representative snapshots of equilibrium configurations for selected states as shown in Fig. 5. It can clearly be seen that at the lowest pressure ($P_N^* = 0.02$), the wall tends to be relative dry of the rod particles, while a planar anchoring is noticeable at $P_N^* = 0.20$. At the higher pressure of $P_N^* = 0.90$, the system is seen to exhibit surface nematization before experiencing a bulk isotropic-nematic transition at $P_N^* \sim 1.14$.

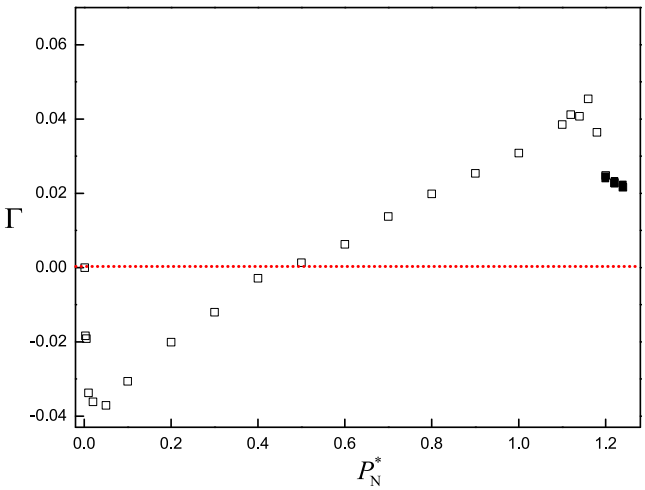

FIG. 4. Surface adsorption as a function of the equilibrium (normal) pressure P_N^* for a system of pure $L/D = 5$ hard spherocylinders confined between parallel hard walls obtained from NP_NT-MC simulations. The open squares correspond to bulk isotropic states, the filled squares correspond to bulk nematic states, and the dashed red curve denotes zero net adsorption.

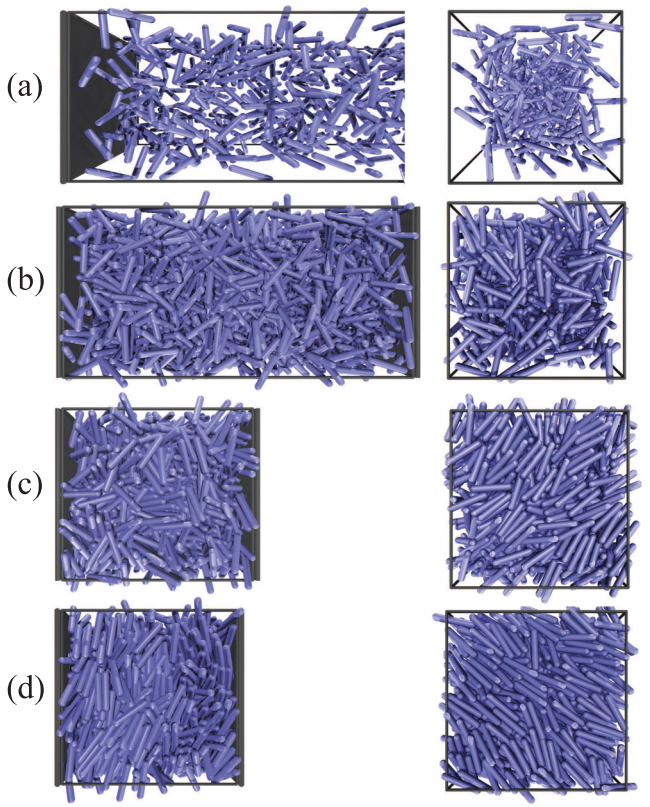

FIG. 5. Representative configurations for a system of pure $L/D = 5$ hard spherocylinders confined between parallel hard walls obtained from NP_NT-MC simulations at equilibrium (normal) pressures of: (a) $P_N^* = 0.02$; (b) $P_N^* = 0.20$; (c) $P_N^* = 0.90$; and (d) $P_N^* = 1.14$. The configurations are shown in the direction parallel to the hard walls (the *xy* plane) on the left and in the direction perpendicular to the hard walls (along the *z* direction) on the right.

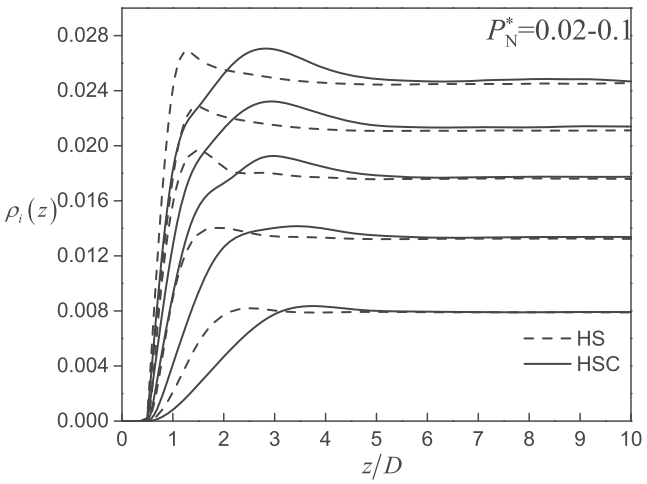

FIG. 6. Density profiles $\rho_i(z)$ of a binary equimolar mixture ($x_{HS} = 0.5$) of $L/D = 5$ hard spherocylinders (HSC, continuous curves) and hard spheres (HS, dashed curves) confined between parallel hard walls obtained from NP_NT-MC simulations. The various curves correspond to states with different equilibrium (normal) pressures of $P^*_N = [0.02 - 0.1]$ (from bottom to top) with increments of $\Delta P^*_N = 0.02$.

B. Binary mixtures of hard spherocylinders and hard spheres in planar confinement between hard walls

We are now in a position to study the influence of hard spheres on the surface behavior of binary mixtures of hard spherocylinders and hard spheres. The case of the equimolar mixture ($x_{HS} = 0.5$) is considered first. Density profiles for both species over the pressure range of $P^*_N = [0.02 - 0.1]$ are shown in Fig. 6. As observed in the system of pure hard spherocylinders, these low-pressure isotropic states are characterized by a depletion of rods from the wall that maximizes their orientation entropy. In turn this creates an available volume near the wall that can be occupied by the smaller hard-sphere particles. In view of the isotropic character of the lower-density states, the HSC components essentially behave like hard spheres with an effective diameter of $\sim(L + D)/2$.

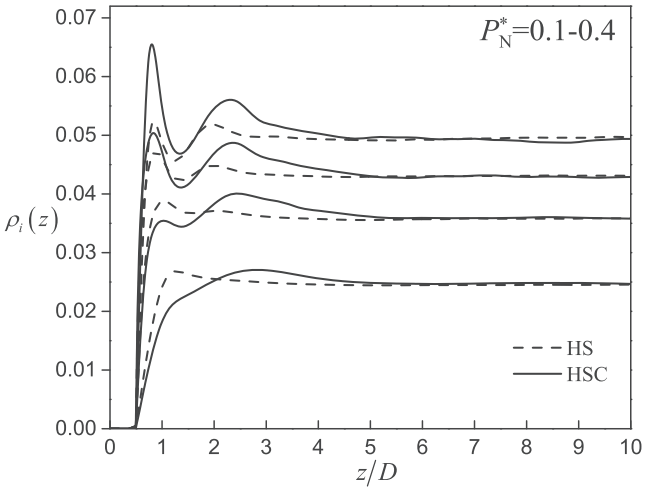

FIG. 7. Density profiles $\rho_i(z)$ of a binary equimolar mixture ($x_{HS} = 0.5$) of $L/D = 5$ hard spherocylinders (HSC, continuous curves) and hard spheres (HS, dashed curves) confined between parallel hard walls obtained from NP_NT-MC simulations. The various curves correspond to states for different equilibrium (normal) pressures of $P^*_N = [0.1, 0.2, 0.3, 0.4]$ (bottom to top).

Consequently, the hard spheres are preferentially adsorbed at the wall and the corresponding density profiles exhibit a weak peak at $z \sim D$, while a peak in the density profiles of hard spherocylinders develops at $z \sim 3D$. The density profiles for the intermediate pressure range of $P^*_N = [0.1 - 0.4]$ are shown in Fig. 7. As the pressure is increased, a new peak adjacent to the wall ($z \sim D/2$) develops in the density profile of the hard spherocylinders which exceeds the one for hard spheres for pressures $P^*_N > 0.2$ and can be attributed to the onset of surface nematization and planar anchoring. As the pressure is further increased, the second peak in the density profile for the rods moves toward the wall from $z \sim 3D$ to $z \sim 2D$ due to propagation of the nematic ordering away from the wall; the density profiles for the hard spherocylinders are now

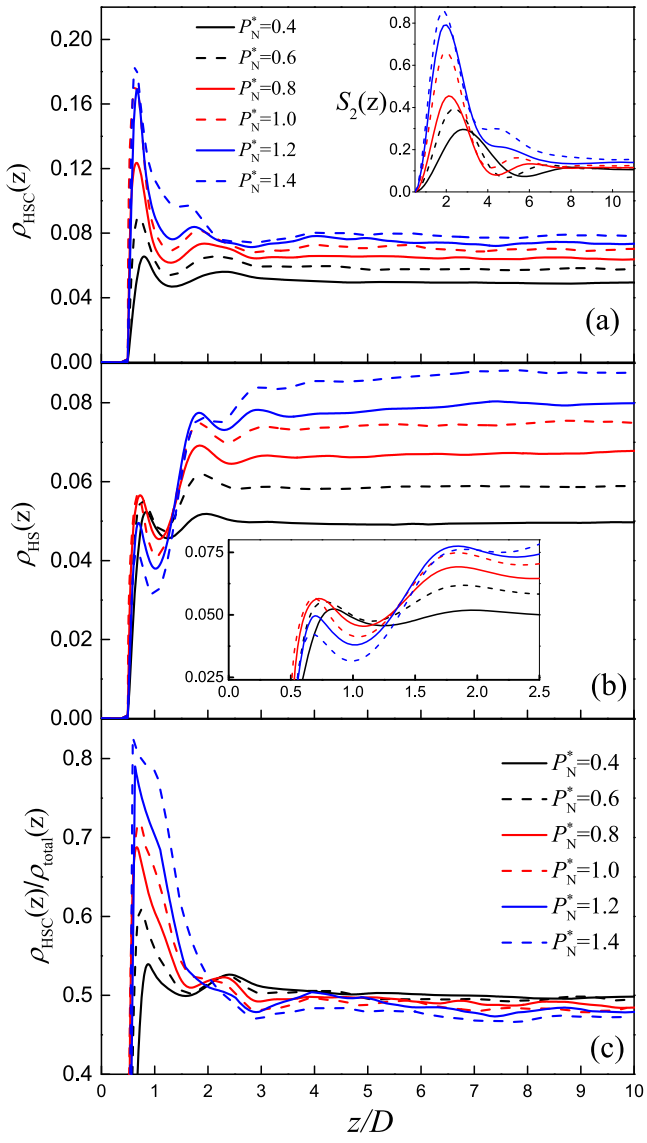

FIG. 8. Density profiles $\rho_i(z)$ of (a) $L/D = 5$ hard spherocylinders and (b) hard spheres in a binary equimolar mixture ($x_{HS} = 0.5$) confined between parallel hard walls obtained from NP_NT-MC simulations. The various curves correspond to states for different equilibrium (normal) pressures of $P^*_N = [0.4 - 1.4]$ (bottom to top). The nematic order parameter profiles $S_2(z)$ of the hard spherocylinders are shown in the inset of (a). The behavior of the density profiles for hard spheres near a hard wall is highlighted in the inset of (b). (c) The corresponding composition profiles $x_{HSC}(z) = \rho_{HSC}(z)/\rho_{total}(z)$.

seen to exhibit oscillations with a periodicity of D rather than $(L + D)/2$. The enhancement of surface nematization by the rods leads to the spheres being pushed away from the wall, resulting in a reduction of the hard-sphere density near the wall reflected by the progressively weaker amplitude of the first peak.

The behavior of the equimolar mixture of hard spherocylinders and hard spheres at higher equilibrium (normal) pressures in the range $P_N^* = [0.4 - 1.4]$ is shown in Fig. 8. It is clear from the density profiles that the orientational ordering of the rods near the wall is enhanced at higher pressure as reflected in the behavior of the nematic order parameter which is seen to increase significantly near the wall. In this high-pressure regime, we observe the onset of a surface nematization, although at a somewhat higher pressure ($P_N^* \sim 1.0$) than in the case of the pure hard-spherocylinder system ($P_N^* \sim 0.7$), demonstrating that the presence of hard spheres destabilizes the nematic ordering of the rods. The surface nematization leads to even stronger depletion of the hard spheres from the wall than in the low-pressure regime, which leads to local demixing of the fluid.

The behavior of the binary mixture can also be analyzed by examining the surface adsorption of the hard spherocylinders (Γ_{HSC}) and hard spheres (Γ_{HS}) calculated using Eq. (3) as depicted in Fig. 9. At low pressures, the adsorption is negative for both components, with the adsorption of hard spheres just slightly higher than that of the hard spherocylinders. However, a crossover in adsorption is observed at a pressure of $P_N^* \sim 0.16$ beyond which the rods are preferentially adsorbed. This behavior is a consequence of the spheres being excluded from the region close to the wall due to the reorientation of the rods forming the first nematic layer. As the pressure is further increased, the preferential adsorption of hard spherocylinders becomes more evident leading eventually to a local demixing of the mixture. Representative snapshots of equilibrium configurations for equilibrium (normal) pressures ranging from low-density isotropic states to the high-density nematic states are shown in Fig. 10. The planar configuration of the rods in the high-density state is clearly apparent.

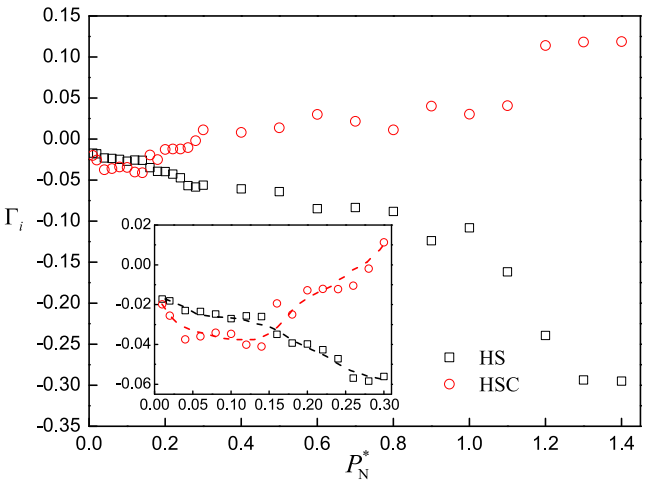

FIG. 9. Surface adsorption Γ_i (i = HSC, HS) of a binary equimolar mixture ($x_{HS} = 0.5$) of $L/D = 5$ hard spherocylinders (HSC, circles) and hard spheres (HS, squares) confined between parallel hard walls as a function of the equilibrium (normal) pressure P_N^* obtained from NP_NT-MC simulations. The competing adsorption between the rods and spheres is highlighted in the inset. Dashed curves are drawn to guide the eye.

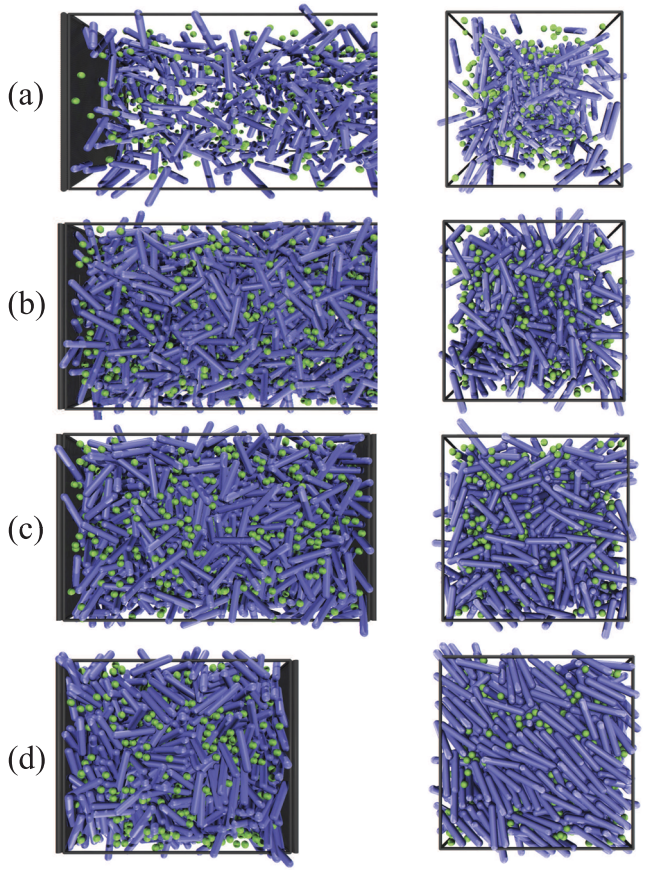

FIG. 10. Representative configurations for a binary equimolar mixture ($x_{HS} = 0.5$) of $L/D = 5$ hard spherocylinders and hard spheres confined between parallel hard walls obtained from NP_NT-MC simulations at equilibrium (normal) pressures of: (a) $P_N^* = 0.04$; (b) $P_N^* = 0.26$; (c) $P_N^* = 0.60$; and (d) $P_N^* = 1.40$. The configurations are shown in the direction parallel to the hard wall (the xy plane) on the left and in the direction perpendicular to the hard wall (along the z direction) on the right.

It has been shown previously[88] that the presence of spherical particles in a system of rod-like particles destabilizes the formation of the bulk nematic phase. Here, we analyze the impact of the presence of hard spheres on the formation of nematic films near a hard wall in binary mixtures of hard spherocylinders and hard spheres with different compositions. As shown in Fig. 11 thick nematic films adsorb at the walls for mixtures with compositions of $x_{HS} = 0$, 0.1, 0.2, and 0.5 at a fixed equilibrium (normal) pressure of $P_N^* = 1.0$. The thickness and the orientational order of the nematic layer are both seen to decrease as the composition of spheres is decreased. We can, therefore, conclude that not only the bulk isotropic-nematic transition but also the surface nematization is destabilized by the presence of hard spheres.

Based on the previous findings, one might expect that the presence of high concentrations of hard spheres would weaken the preferential adsorption of rods in favour of spheres. This is, however, not the case as inferred from the dependence of the surface adsorption on the hard-sphere composition presented in Fig. 12. Here, we introduce the quantity $\Delta_W = \Gamma_{HSC} - \Gamma_{HS}$ characterizing the relative adsorption of

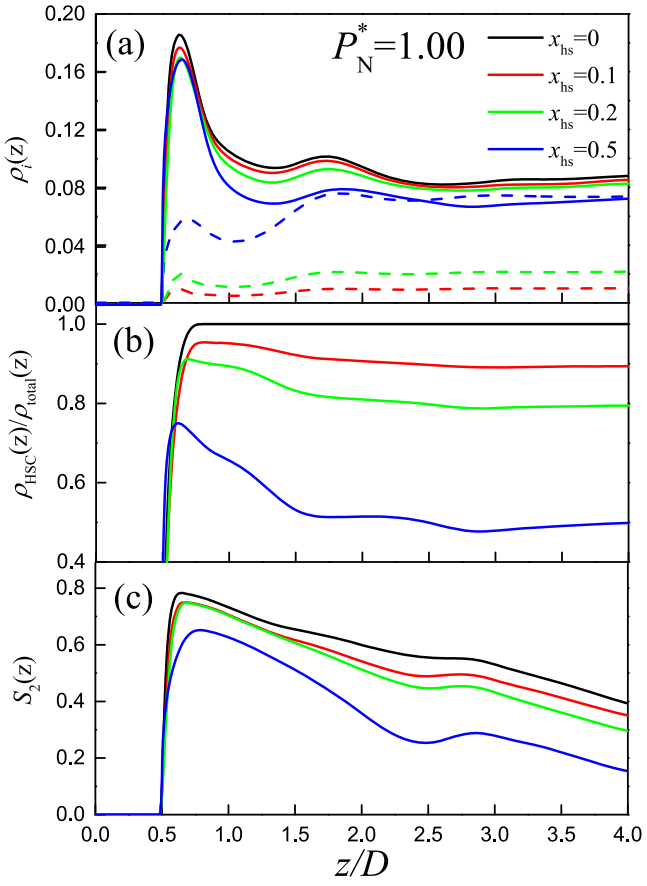

FIG. 11. (a) Density profiles $\rho_i(z)$, (b) concentration profiles $x_{HSC}(z) = \rho_{HSC}(z)/\rho_{total}(z)$, and (c) nematic order parameter profiles $S_2(z)$ for mixtures of L/D = 5 hard spherocylinders and hard spheres confined between parallel hard walls obtained from NP_NT-MC simulations with varying overall hard-sphere composition x_{HS} at a fixed equilibrium (normal) pressure of P_N^* = 1.0. The continuous curves in (a) represent the density profiles of the hard spherocylinders and the dashed curves are those for the hard spheres.

the hard spherocylinders with respect to that of the hard spheres. It is apparent that as the hard-sphere concentration is increased, the adsorption of the hard spherocylinders is largely unaffected, while the adsorption of the hard spheres decreases rather dramatically which is a consequence of depletion of the spheres from the walls due to surface induced nematic ordering of the rods. The extent of local demixing near the wall therefore becomes stronger as the concentration of the hard spheres in the mixture is increased. For low concentrations of hard spheres, the effect of the presence of hard spheres is insignificant in terms of adsorption of hard spherocylinders in the nematic layer since the hard spheres are depleted from the wall in the high-pressure regime. It is only when $x_{hs} \sim 0.5$ that the presence of hard spheres can influence the order parameter appreciably.

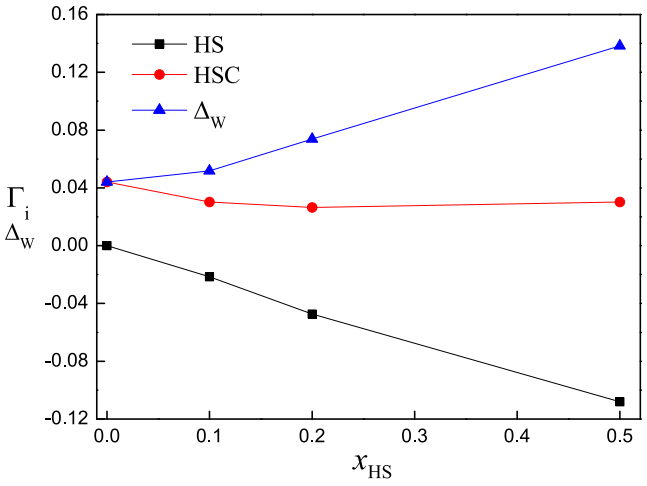

FIG. 12. Dependence of surface adsorption on the overall hard-sphere composition x_{HS} for mixtures of L/D = 5 hard spherocylinders and hard spheres confined between parallel hard walls obtained from NP_NT-MC simulations at a fixed equilibrium (normal) pressure of P_N^* = 1.0. The trend for the differential adsorption $\Delta_W = \Gamma_{HSC} - \Gamma_{HS}$ is also included.

IV. CONCLUSIONS

We have studied the structure, orientational ordering, and phase behavior of pure hard spherocylinders and of binary mixtures of hard spherocylinders and hard spheres confined between parallel hard walls using constant normal-pressure MC simulations. The aspect ratio of the hard spherocylinders considered is L/D = 5 and the hard-sphere diameter is taken to be the same as the cylinder diameter D. States up to the bulk isotropic-nematic transition are examined.

Starting with surface properties of pure rods, we find that at low-pressure (low-density) states, the system is fully isotropic resulting in a depletion of the particles from the hard walls in order to maximize the (dominant) contribution to the orientational entropy. At higher pressures, packing effects prevail and the rods adsorb at the wall with a near-linear dependence of the adsorption with pressure. This process is accompanied by a surface nematization with the nematic director oriented parallel to the wall and the induced nematic film growing continuously up to the bulk isotropic-nematic transition.

The main objective of our study is to undertake a detailed examination of the effect of the surface on the properties of binary mixtures of rod-like and spherical particles. Here, the competition between the orientational entropy and packing effects near the wall leads to a local demixing of the mixture. At low pressures (densities), we observe a preferential adsorption of hard spheres that fill the free volume left by the rods near the wall from which the rods are depleted due to orientational entropy effects. This effect is, however, quite mild. At higher pressures, a crossover in the preferential surface adsorption occurs beyond which the local demixing near the wall is seen to increase with the pressure. In this regime, the rod particles adsorb at the wall to form a nematic film the width of which increases continuously as the isotropic-nematic transition is approached. The process is accompanied by an increase in the nematic order parameter and depletion of the hard-sphere particles from the walls which in turn leads to local demixing. This process is continuous as we only consider states (pressures) corresponding to bulk isotropic phases. Sudden changes in the structure of the fluid are expected for even higher pressures which exceed the isotropic-nematic transition, as is observed in Fig. 4 for the pure component hard-spherocylinder system. Overall, however, one can conclude that the presence of hard spheres is found to destabilize the surface nematization and an increase in the concentration of hard sphere enhances demixing.

In our current work, we focus exclusively on isotropic and nematic states. Smectic order of rod particles in confinement[28] and layering in rod-sphere mixtures[112] are examples of other surface induced structures occurring at higher pressures. A feature which has been omitted in our study is an analysis of the expected biaxiality and of the rod-like particles close to the wall and the fluid-wall interfacial tension.[33,57,58] The method adopted in our current study to characterize the spatial distribution of the order parameter tensor is not sufficiently accurate to compute the biaxiality of HSCs induced by the surface. We postpone this to future work, and we also plan to use advanced DFT methodologies[12,85,113] to predict the surface behavior of mixtures of rods and spheres including a detailed comparison with simulation. It is also important to add that Koga *et al.*[114] have reported a related study of mixtures of hard spherocylinders and hard spheres in planar confinement with a wall-sphere attractive potential; in this case the spheres fully adsorb on the walls owing to the strength of the wall-sphere potential, and the rod-like particles behave in a similar fashion to the confined pure component hard-spherocylinder system.

ACKNOWLEDGMENTS

L.W. thanks the Department for Business Innovation and Skills of the UK and China Scholarship Council for funding a Ph.D. studentship. The MC simulations were performed using the High Performance Computing service provided by Imperial College London. A.M. acknowledges support from the Czech Science Foundation, Project No. 16-12291S. Funding to the Molecular Systems Engineering Group from the Engineering and Physical Sciences Research Council (EPSRC) of the UK (Grant Nos. GR/T17595, GR/N35991, EP/E016340, and EP/J014958), the Joint Research Equipment Initiative (JREI) (No. GR/M94426), and the Royal Society-Wolfson Foundation refurbishment scheme is also gratefully acknowledged.

[1]F. A. Escobedo, "Engineering entropy in soft matter: The bad, the ugly and the good," Soft Matter **10**, 8388–8400 (2014).
[2]V. N. Manoharan, "Colloidal matter: Packing, geometry, and entropy," Science **349**, 1253751 (2015).
[3]S. C. Glotzer and M. J. Solomon, "Anisotropy of building blocks and their assembly into complex structures," Nat. Mater. **6**, 557–562 (2007).
[4]P. F. Damasceno, M. Engel, and S. C. Glotzer, "Predictive self-assembly of polyhedra into complex structures," Science **337**, 453–457 (2012).
[5]G. van Anders, N. K. Ahmed, R. Smith, M. Engel, and S. C. Glotzer, "Entropically patchy particles: Engineering valence through shape entropy," ACS Nano **8**, 931–940 (2014).
[6]C. Avendaño, G. Jackson, E. A. Müller, and F. A. Escobedo, "Assembly of porous smectic structures formed from interlocking high-symmetry planar nanorings," Proc. Natl. Acad. Sci. U. S. A. **113**, 9699–9703 (2016).
[7]C. Avendaño and F. A. Escobedo, "Packing, entropic patchiness, and self-assembly of non-convex colloidal particles: A simulation perspective," Curr. Opin. Colloid Interface Sci. **30**, 62–69 (2017).
[8]A. Yethiraj and A. van Blaaderen, "A colloidal model system with an interaction tunable from hard sphere to soft and dipolar," Nature **421**, 513–517 (2003).
[9]L. Onsager, "The effects of shape on the interaction of colloidal particles," Ann. N. Y. Acad. Sci. **51**, 627–659 (1949).
[10]D. Frenkel, "Onsager's spherocylinders revisited," J. Phys. Chem. **91**, 4912–4916 (1987).
[11]S. C. McGrother, D. C. Williamson, and G. Jackson, "A re-examination of the phase diagram of hard spherocylinders," J. Chem. Phys. **104**, 6755–6771 (1996).
[12]H. Hansen-Goos and K. Mecke, "Fundamental measure theory for inhomogeneous fluids of nonspherical hard particles," Phys. Rev. Lett. **102**, 018302 (2009).
[13]P. G. Bolhuis and D. Frenkel, "Tracing the phase boundaries of hard spherocylinders," J. Chem. Phys. **106**, 666–687 (1997).
[14]H. Löwen, "Colloidal dispersions in external fields: Recent developments," J. Phys.: Condens. Matter **20**, 404201 (2008).
[15]R. Evans, U. M. B. Marconi, and P. Tarazona, "Fluids in narrow pores: Adsorption, capillary condensation, and critical points," J. Chem. Phys. **84**, 2376 (1986).
[16]B. Jérôme, "Surface effects and anchoring in liquid crystals," Rep. Prog. Phys. **54**, 391–451 (1991).
[17]T. J. Sluckin, "Anchoring transitions at liquid crystal surfaces," Phys. A **213**, 105–109 (1995).
[18]P. Sheng, "Phase transition in surface-aligned nematic films," Phys. Rev. Lett. **37**, 1059–1062 (1976).
[19]M. M. Telo da Gama, "The interfacial properties of a model of a nematic liquid-crystal. 1. The nematic-isotropic and the nematic-vapor interfaces," Mol. Phys. **52**, 585–610 (1984).
[20]M. M. Telo da Gama, "The interfacial properties of a model of a nematic liquid-crystal. 2. Induced orientational order and wetting transitions at a solid fluid interface," Mol. Phys. **52**, 611–630 (1984).
[21]M. M. Telo da Gama, P. Tarazona, M. P. Allen, and R. Evans, "The effect of confinement on the isotropic nematic transition," Mol. Phys. **71**, 801–821 (1990).
[22]A. Poniewierski and T. J. Sluckin, "Statistical-mechanics of a simple-model of the nematic liquid crystal-wall interface," Mol. Cryst. Liq. Cryst. **111**, 373–386 (1984).
[23]A. Poniewierski and T. J. Sluckin, "Theory of the nematic-isotropic transition in a restricted geometry," Liq. Cryst. **2**, 281–311 (1987).
[24]A. Poniewierski and R. Hołyst, "Nematic alignment at a solid substrate: The model of hard spherocylinders near a hard wall," Phys. Rev. A **38**, 3721–3727 (1988).
[25]A. Poniewierski, "Ordering of hard needles at a hard wall," Phys. Rev. E **47**, 3396 (1993).
[26]R. van Roij, M. Dijkstra, and R. Evans, "Interfaces, wetting, and capillary nematization of a hard-rod fluid: Theory for Zwanzig model," J. Chem. Phys. **113**, 7689–7701 (2000).
[27]R. Aliabadi, M. Moradi, and S. Varga, "Orientational ordering of confined hard rods: The effect of shape anisotropy on surface ordering and capillary nematization," Phys. Rev. E **92**, 032503 (2015).
[28]A. Malijevský and S. Varga, "Phase behaviour of parallel hard rods in confinement: An Onsager theory study," J. Phys.: Condens. Matter **22**, 175002 (2010).
[29]S. Ye, P. Zhang, and J. Z. Y. Chen, "Surface-induced phase transitions of wormlike chains in slit confinement," Soft Matter **12**, 2948–2959 (2016).
[30]L. Qin and J. Z. Y. Chen, "Recent theoretical development in confined liquid-crystal polymers," Acta Phys. Sin. **65**, 174201 (2016).
[31]Y. Mao, M. E. Cates, and H. N. W. Lekkerkerker, "Theory of the depletion force due to rodlike polymer," J. Chem. Phys. **106**, 3721–3729 (1997).
[32]Y. Mao, P. Bladon, H. N. W. Lekkerkerker, and M. E. Cates, "Density profiles and thermodynamics of rod-like particles between parallel walls," Mol. Phys. **92**, 151–159 (1997).
[33]M. Dijkstra, R. van Roij, and R. Evans, "Wetting and capillary nematization of a hard-rod fluid: A simulation study," Phys. Rev. E. **63**, 051703 (2001).
[34]D. de las Heras, E. Velasco, and L. Mederos, "Effects of wetting and anchoring on capillary phenomena in a confined liquid crystal," J. Chem. Phys. **120**, 4949–4957 (2004).
[35]M. Dijkstra and R. van Roij, "Entropic wetting in colloidal particles," J. Phys.: Condens. Matter **17**, S3507–S3514 (2005).
[36]S. Jungblut, R. Tuinier, K. Binder, and T. Schilling, "Depletion induced isotropic-isotropic phase separation in suspensions of rod-like colloids," J. Chem. Phys. **127**, 244909 (2007).
[37]M. P. Allen, "Molecular simulation and theory of liquid crystal surface anchoring," Mol. Phys. **96**, 1391–1397 (1999).
[38]M. P. Allen, "Molecular simulation and theory of the isotropic-nematic interface," J. Chem. Phys. **112**, 5447–5453 (2000).
[39]M. M. Piñeiro, A. Galindo, and A. O. Parry, "Surface ordering and capillary phenomena of confined hard cut-sphere particles," Soft Matter **3**, 768–778 (2007).
[40]C. Avendaño, C. M. Liddell Watson, and F. A. Escobedo, "Directed self-assembly of spherical caps via confinement," Soft Matter **9**, 9153–9166 (2013).

[41]K. Muangnapoh, C. Avendaño, F. A. Escobedo, and C. M. Liddell Watson, "Degenerate crystals from colloidal dimers under confinement," Soft Matter **10**, 9729–9738 (2014).

[42]F. Barmes and D. J. Cleaver, "Computer simulation of a liquid-crystal anchoring transition," Phys. Rev. E **69**, 061705 (2004).

[43]T. Gruhn and M. Schoen, "Substrate-induced order in confined nematic liquid-crystal films," J. Chem. Phys. **108**, 9124–9136 (1998).

[44]E. A. Müller, I. Rodríguez-Ponce, A. Oualid, J. M. Romero-Enrique, and L. F. Rull, "Wetting of planar surfaces by a Gay-Berne liquid crystal," Mol. Simul. **29**, 385–391 (2003).

[45]L. F. Rull, J. M. Romero-Enrique, and E. A. Müller, "Observation of surface nematization at the solid-liquid crystal interface via molecular simulation," J. Phys. Chem. C **111**, 15998–16005 (2007).

[46]Q. Ji, R. Lefort, and D. Morineau, "Influence of pore shape on the structure of a nanoconfined Gay-Berne liquid crystal," Chem. Phys. Lett. **478**, 161–165 (2009).

[47]M. Greschek and M. Schoen, "Orientational prewetting of planar solid substrates by a model liquid crystal," J. Chem. Phys. **135**, 204702 (2011).

[48]V. A. Ivanov, A. S. Rodionova, J. A. Martemyanova, M. R. Stukan, M. Müller, W. Paul, and K. Binder, "Wall-induced orientational order in athermal semidilute solutions of semiflexible polymers: Monte Carlo simulations of a lattice model," J. Chem. Phys. **138**, 234903 (2013).

[49]V. A. Ivanov, A. S. Rodionova, J. A. Martemyanova, M. R. Stukan, M. Müller, W. Paul, and K. Binder, "Conformational properties of semiflexible chains at nematic ordering transitions in thin films: A Monte Carlo simulation," Macromolecules **47**, 1206–1220 (2014).

[50]A. Milchev, S. A. Egorov, and K. Binder, "Semiflexible polymers confined in a slit pore with attractive walls: Two-dimensional liquid crystalline order versus capillary nematization," Soft Matter **13**, 1888–1903 (2017).

[51]S. A. Egorov, A. Milchev, and K. Binder, "Capillary nematization of semiflexible polymers," Macromol. Theory Simul. **26**, 1600036 (2017).

[52]S. Varga and G. Jackson, "Simulation of the macroscopic pitch of a chiral nematic phase of a model chiral mesogen," Chem. Phys. Lett. **377**, 6–12 (2003).

[53]S. Varga and G. Jackson, "Study of the pitch of fluids of electrostatically chiral anisotropic molecules: Mean-field theory and simulation," Mol. Phys. **104**, 3681–3691 (2006).

[54]D. L. Cheung and F. Schmid, "Monte Carlo simulations of liquid crystals near rough walls," J. Chem. Phys. **122**, 074902 (2005).

[55]H. Steuer, S. Hess, and M. Schoen, "Phase behavior of liquid crystals confined by smooth walls," Phys. Rev. E **69**, 031708 (2004).

[56]Y. Trukhina and T. Schilling, "Computer simulation study of a liquid crystal confined to a spherical cavity," Phys. Rev. E **77**, 011701 (2008).

[57]P. E. Brumby, A. J. Haslam, E. de Miguel, and G. Jackson, "Subtleties in the calculation of the pressure and pressure tensor of anisotropic particles from volume-perturbation methods and the apparent asymmetry of the compressive and expansive contributions," Mol. Phys. **109**, 169–189 (2011).

[58]P. E. Brumby, H. H. Wensink, A. J. Haslam, and G. Jackson, "Structure and interfacial tension of a hard-rod fluid in planar confinement," Langmuir **33**, 11754–11770 (2017).

[59]S. V. Savenko and M. Dijkstra, "Sedimentation and multiphase equilibria in suspensions of colloidal hard rods," Phys. Rev. E **70**, 051401 (2004).

[60]H. Zocher, Z. Anorg. Allg. Chem. **147**, 91 (1925).

[61]F. M. van der Kooij, K. Kassapidou, and H. N. W. Lekkerkerker, "Liquid crystal phase transitions in suspensions of polydisperse plate-like particles," Nature **406**, 868 (2000).

[62]H. H. Wensink and H. N. W. Lekkerkerker, "Phase diagram of hard colloidal platelets: A theoretical account," Mol. Phys. **107**, 2111–2118 (2009).

[63]M. Bravo-Sanchez, T. J. Simmons, and M. A. Vidal, "Liquid crystal behavior of single wall carbon nanotubes," Carbon **48**, 3531–3542 (2010).

[64]R. Mezzenga, J.-M. Jung, and J. Adamcik, "Effects of charge double layer and colloidal aggregation on the isotropic-nematic transition of protein fibers in water," Langmuir **26**, 10401–10405 (2010).

[65]V. A. Parsegian and S. L. Brenner, "The role of long range forces in ordered arrays of tobacco mosaic virus," Nature **259**, 632–635 (1976).

[66]Z. Dogic and S. Fraden, "Smectic phase in a colloidal suspension of semiflexible virus particles," Phys. Rev. Lett. **78**, 2417–2420 (1997).

[67]K. R. Purdy, S. Varga, A. Galindo, G. Jackson, and S. Fraden, "Nematic phase transitions in mixtures of thin and thick colloidal rods," Phys. Rev. Lett. **94**, 057801 (2005).

[68]W. G. Miller, C. C. Wu, E. L. Wee, G. L. Santee, J. H. Rai, and K. G. Goebel, "Thermodynamics and dynamics of polypeptide liquid crystals," Pure Appl. Chem. **38**, 37–58 (1974).

[69]J. C. Horton, A. M. Donald, and A. Hill, "Coexistence of two liquid crystalline phases in poly(benzyl-l-glutamate) solutions," Nature **346**, 44–45 (1990).

[70]M. Nakata, G. Zanchetta, B. D. Chapman, C. D. Jones, J. O. Cross, R. Pindak, T. Bellini, and N. A. Clark, "End-to-end stacking and liquid crystal condensation of 6-to 20-base pair DNA duplexes," Science **318**, 1276–1279 (2007).

[71]J. Galanis, D. Harries, D. L. Sackett, W. Losert, and R. Nossal, "Spontaneous patterning of confined granular rods," Phys. Rev. Lett. **96**, 028002 (2006).

[72]A. Kuijk, D. V. Byelov, A. V. Petukhov, A. van Blaaderen, and A. Imhof, "Phase behavior of colloidal silica rods," Faraday Discuss. **159**, 181–199 (2012).

[73]A. Stroobants, H. N. W. Lekkerkerker, and D. Frenkel, "Evidence for smectic order in a fluid of hard parallel spherocylinders," Phys. Rev. Lett. **57**, 1452–1455 (1986).

[74]D. Frenkel, H. N. W. Lekkerkerker, and A. Stroobants, "Thermodynamic stability of a smectic phase in a system of hard rods," Nature **332**, 822–823 (1988).

[75]J. A. C. Veerman and D. Frenkel, "Phase diagram of a system of hard spherocylinders by computer simulation," Phys. Rev. A **41**, 3237–3244 (1990).

[76]M. P. Allen, G. T. Evans, D. Frenkel, and B. M. Mulder, "Hard convex body fluids," Adv. Chem. Phys. **86**, 1–166 (1993).

[77]H. N. W. Lekkerkerker, P. Coulon, R. V. D. Haegen, and R. Deblieck, "On the isotropic liquid crystal phase separation in a solution of rodlike particles of different lengths," J. Chem. Phys. **80**, 3427–3433 (1984).

[78]T. Odijk and H. N. W. Lekkerkerker, "Theory of the isotropic-liquid crystal phase separation for a solution of bidisperse rodlike macromolecules," J. Phys. Chem. **89**, 2090–2096 (1985).

[79]R. van Roij and B. Mulder, "Absence of high-density consolute point in nematic hard rod mixtures," J. Chem. Phys. **105**, 11237–11245 (1996).

[80]S. Varga, K. Purdy, A. Galindo, S. Fraden, and G. Jackson, "Nematic-nematic phase separation in binary mixtures of thick and thin hard rods: Results from Onsager-like theories," Phys. Rev. E **72**, 051704 (2005).

[81]P. G. Bolhuis and D. Frenkel, "Numerical study of the phase diagram of a mixture of spherical and rodlike colloids," J. Chem. Phys. **101**, 9869–9875 (1994).

[82]G. A. Vliegenthart and H. N. W. Lekkerkerker, "Phase behavior of colloidal rod-sphere mixtures," J. Chem. Phys. **111**, 4153–4157 (1999).

[83]G. H. Koenderink, G. A. Vliegenthart, S. G. J. M. Kluijtmans, A. van Blaaderen, A. P. Philipse, and H. N. W. Lekkerkerker, "Depletion-induced crystallization in colloidal rod-sphere mixtures," Langmuir **15**, 4693–4696 (1999).

[84]M. Schmidt, "Density functional theory for colloidal rod-sphere mixtures," Phys. Rev. E **63**, 050201 (2001).

[85]R. Roth, J. M. Brader, and M. Schmidt, "Entropic wetting of a colloidal rod-sphere mixture," Europhys. Lett. **63**, 549–555 (2003).

[86]M. Schmidt and J. M. Brader, "Hard sphere fluids in random fiber networks," J. Chem. Phys. **119**, 3495–3500 (2003).

[87]N. Urakami and M. Imai, "Dependence on sphere size of the phase behavior of mixtures of rods and spheres," J. Chem. Phys. **119**, 2463–2470 (2003).

[88]S. Lago, A. Cuetos, B. Martínez-Haya, and L. F. Rull, "Crowding effects in binary mixtures of rod-like and spherical particles," J. Mol. Recognit. **17**, 417–425 (2004).

[89]A. Cuetos, B. Martínez-Haya, S. Lago, and L. F. Rull, "Use of Parsons-Lee and Onsager theories to predict nematic and demixing behavior in binary mixtures of hard rods and hard spheres," Phys. Rev. E **75**, 061701 (2007).

[90]G. Cinacchi and L. D. Gaetani, "Diffusion in the lamellar phase of a rod-sphere mixture," J. Chem. Phys. **131**, 104908 (2009).

[91]L. Wu, A. Malijevský, G. Jackson, E. A. Müller, and C. Avendaño, "Orientational ordering and phase behaviour of binary mixtures of hard spheres and hard spherocylinders," J. Chem. Phys. **143**, 044906 (2015).

[92]A. Stroobants and H. N. W. Lekkerkerker, "Liquid crystal phase transitions in a solution of rodlike and disklike particles," J. Phys. Chem. **88**, 3669–3674 (1984).

[93]A. G. Vanakaras, S. C. McGrother, G. Jackson, and D. J. Photinos, "Hydrogen-bonding and phase biaxiality in nematic rod-plate mixtures," Mol. Cryst. Liq. Cryst. **323**, 199–209 (1998).

[94]F. M. van der Kooij and H. N. W. Lekkerkerker, "Liquid-crystalline phase behavior of a colloidal rod-plate mixture," Phys. Rev. Lett. **84**, 781–784 (2000).

[95]A. Galindo, G. Jackson, and D. J. Photinos, "Computer simulation of the interface between two liquid crystalline phases in rod-plate binary mixtures," Chem. Phys. Lett. **325**, 631–638 (2000).
[96]H. H. Wensink, G. J. Vroege, and H. N. W. Lekkerkerker, "Biaxial versus uniaxial nematic stability in asymmetric rod-plate mixtures," Phys. Rev. E **66**, 041704 (2002).
[97]S. Varga, A. Galindo, and G. Jackson, "Ordering transitions, biaxiality, and demixing in the symmetric binary mixture of rod and plate molecules described with the Onsager theory," Phys. Rev. E **66**, 011707 (2002).
[98]A. Galindo, A. J. Haslam, S. Varga, G. Jackson, A. G. Vanakaras, D. J. Photinos, and D. A. Dunmur, "The phase behavior of a binary mixture of rodlike and disclike mesogens: Monte Carlo simulation, theory, and experiment," J. Chem. Phys. **119**, 5216–5225 (2003).
[99]A. Cuetos, A. Galindo, and G. Jackson, "Thermotropic biaxial liquid crystalline phases in a mixture of attractive uniaxial rod and disk particles," Phys. Rev. Lett. **101**, 237802 (2008).
[100]H. H. Wensink, G. J. Vroege, and H. N. W. Lekkerkerker, "Isotropic-nematic density inversion in a binary mixture of thin and thick hard platelets," J. Phys. Chem. B **105**, 10610–10618 (2001).
[101]A. A. Verhoeff, H. H. Wensink, M. Vis, G. Jackson, and H. N. W. Lekkerkerker, "Liquid crystal phase transitions in systems of colloidal platelets with bimodal shape distribution," J. Phys. Chem. B **113**, 13476–13484 (2009).
[102]F. Gámez, R. D. Acemel, and A. Cuetos, "Demixing and nematic behaviour of oblate hard spherocylinders and hard spheres mixtures: Monte Carlo simulation and Parsons-Lee theory," Mol. Phys. **111**, 3136 (2013).
[103]A. Malijevský, G. Jackson, and S. Varga, "Many-fluid Onsager density functional theories for orientational ordering in mixtures of anisotropic hard-body fluids," J. Chem. Phys. **129**, 144504 (2008).
[104]J. M. Brader, A. Esztermann, and M. Schmidt, "Colloidal rod-sphere mixtures: Fluid-fluid interfaces and the Onsager limit," Phys. Rev. E **66**, 031401 (2002).
[105]P. G. de Gennes and J. Prost, *The Physics of Liquid Crystals*, 2nd ed. (Oxford University Press, Oxford, 1993).
[106]W. H. Press, S. A. Teukolsky, and W. T. Vetterling, *Numerical Recipes in FORTRAN: The Art of Scientific Computing*, 2nd ed. (Cambridge University Press, Cambridge, 1992).
[107]R. Eppenga and D. Frenkel, "Monte-Carlo study of the isotropic and nematic phases of infinitely thin hard platelets," Mol. Phys. **52**, 1303–1334 (1984).
[108]A. Richter and T. Gruhn, "Structure formation and fractionation in systems of polydisperse attractive rods," J. Chem. Phys. **125**, 064908 (2006).
[109]J. R. Henderson and F. van Swol, "On the interface between a fluid and a planar wall: Theory and simulations of a hard-sphere fluid at a hard-wall," Mol. Phys. **51**, 991–1010 (1984).
[110]J. R. Henderson and F. van Swol, "Grand potential densities of wall–liquid drying," J. Chem. Phys. **89**, 5010–5014 (1988).
[111]F. van Swol and J. R. Henderson, "Wetting and drying transitions at a fluid-wall interface: Density-functional theory versus computer simulation," Phys. Rev. A **40**, 2567–2578 (1989).
[112]M. Adams, Z. Dogic, S. Keller, and S. Fraden, "Entropically driven microphase transitions in mixtures of colloidal rods and spheres," Nature **393**, 349–352 (1998).
[113]H. Hansen-Goos and K. Mecke, "Tensorial density functional theory for non-spherical hard-body fluids," J. Phys.: Condens. Matter **22**, 364107 (2010).
[114]T. Koda, M. Uchida, A. Nishioka, O. Haba, K. Yonetake, M. Kwak, Y. Momo, N. Kim, S. Hong, D. Kang, and Y. Choi, "Alignment of hard spherocylinders by hard spheres on substrates," Mol. Cryst. Liq. Cryst. **612**, 24–32 (2015).